

Article

A Three-Dimensional Electrochemical Process for the Removal of Carbamazepine

Luísa Correia-Sá ^{1,†}, Cristina Soares ^{1,†} , Olga Matos Freitas ¹ , Manuela Maria Moreira ¹ , Henri Petrus Antonius Nouws ¹ , Manuela Correia ¹ , Paula Paíga ¹, António José Rodrigues ², Carlos Miguel Oliveira ², Sónia Adriana Figueiredo ^{1,*}  and Cristina Delerue-Matos ¹ 

¹ REQUIMTE/LAQV, Instituto Superior de Engenharia do Porto, Politécnico do Porto, 4200-072 Porto, Portugal; mlsrs@isep.ipp.pt (L.C.-S.); cmdss@isep.ipp.pt (C.S.); omf@isep.ipp.pt (O.M.F.); manuela.moreira@graq.isep.ipp.pt (M.M.M.); han@isep.ipp.pt (H.P.A.N.); mmb@isep.ipp.pt (M.C.); pcpa@isep.ipp.pt (P.P.); cmm@isep.ipp.pt (C.D.-M.)

² VentilaQUA, SA, Antanhol, 3040-575 Coimbra, Portugal; antonio.rodrigues@ventilaqua.com (A.J.R.); carlos.oliveira@ventilaqua.com (C.M.O.)

* Correspondence: saf@isep.ipp.pt

† Both authors contributed equally to this work.

Featured Application: This work will allow the development of an efficient, cost-effective and sustainable solution to be used in the removal of pharmaceutical products from wastewaters. It also will contribute to better theoretical and practical knowledge of the three-dimensional electrochemical process as a solution for wastewater treatment.



Citation: Correia-Sá, L.; Soares, C.; Freitas, O.M.; Moreira, M.M.; Nouws, H.P.A.; Correia, M.; Paíga, P.; Rodrigues, A.J.; Oliveira, C.M.; Figueiredo, S.A.; et al. A Three-Dimensional Electrochemical Process for the Removal of Carbamazepine. *Appl. Sci.* **2021**, *11*, 6432. <https://doi.org/10.3390/app11146432>

Academic Editors: Noori MD Tabish, Athanasia Tekerlekopoulou and Ioanna Vasiliadou

Received: 4 May 2021

Accepted: 3 July 2021

Published: 12 July 2021

Publisher's Note: MDPI stays neutral with regard to jurisdictional claims in published maps and institutional affiliations.



Copyright: © 2021 by the authors. Licensee MDPI, Basel, Switzerland. This article is an open access article distributed under the terms and conditions of the Creative Commons Attribution (CC BY) license (<https://creativecommons.org/licenses/by/4.0/>).

Abstract: The scientific community is increasingly concerned about the presence of pharmaceuticals in the aquatic environment, which is a consequence of their high consumption and inefficient removal by wastewater-treatment plants. The search for an effective and sustainable tertiary treatment is therefore needed to enhance their removal. For this purpose, the combination of electrochemical and adsorption processes into three-dimensional (3D) electrochemical systems has been proposed. In this study, a 3D system was studied to remove carbamazepine, an antiepileptic, consumed in high doses and very persistent in the environment. The influences of the following parameters on its removal were evaluated: anode and cathode materials and distance between them, electrolyte (NaCl) concentration and pH, and the (carbon-based) adsorbent material used as the particulate electrode. The obtained results demonstrated that the introduction of the particulate electrode improved the removal efficiency. This can be attributed to the simultaneous occurrence of different phenomena, such as adsorption/electrosorption, electrocoagulation, oxidation, and catalytic degradation.

Keywords: adsorption; advanced oxidation techniques; biochar; pharmaceuticals; stainless steel cathode; mixed metal oxide anode; wastewater treatment

1. Introduction

Human and veterinary pharmaceutical residues from households, wastewater treatment plants, hospitals, industrial units, and intensive animal-breeding farms have been detected in many environmental compartments worldwide. It is well known that the main route of introduction of human pharmaceuticals into the aquatic environment is through the effluents of wastewater-treatment plants (WWTPs) that receive sewage from households and hospitals. As WWTPs were not designed to remove pharmaceuticals, many of these compounds are frequently detected in WWTP effluents at levels ranging from sub-ng/L up to several µg/L [1]. The release of pharmaceuticals into rivers and lakes is becoming an alarming issue because they are a threat to the health of living beings, including humans [2–8]. Groundwater contamination has also been reported. This is primarily due to infiltration of surface water containing pharmaceutical residues and leaks in landfill sites and sewer drains [9–12].

The most hydrophilic pharmaceuticals enter the aquatic environment, and the most hydrophobic ones remain adsorbed on solid particles, sludge from WWTP, or river sediments. Treated wastewater and WWTP sludge (biosolids) are frequently used in the agro-ecosystem [13], contributing to the spread of the contamination. Hence, pharmaceuticals have been recognized as emerging pollutants, and their potential adverse effects on nontarget organisms have been attracting increasing attention [14].

One of the pharmaceuticals ubiquitously present in raw wastewater (ranging from ng/L to µg/L) and poorly removed by conventional WWTPs [15] is carbamazepine (CBZ), which is an anticonvulsant and mood-stabilizing drug, primarily used in the treatment of epilepsy and bipolar disorder, and consumed in substantial daily amounts (daily dose of 1000 mg for epilepsy treatment) [16,17]. Approximately 30% of the oral CBZ dosage is excreted in its nonconjugated form in urine and feces [17]. In this context, CBZ has been proposed as an anthropogenic marker of sewage contamination in freshwater bodies due to its persistence and presence in waters [18]. Its adverse effects on several species have been demonstrated; CBZ can be assimilated and bioaccumulated in cucumber plants [19], and may produce oxidative stress in the common carp [20]. Although its occurrence in freshwater may not pose an immediate threat to aquatic ecosystems or human health, effective removal of CBZ is still required for safe water reuse. The presence of CBZ in the water cycle has increased the concern about its removal in WWTPs.

During primary wastewater treatment, adsorption on primary sludge is the main mechanism of removal. However, due to the low log octanol–water partition coefficient (K_{ow}) values of CBZ (low hydrophobicity), it is not expected to be adsorbed significantly onto sludge, but instead to dissociate in the aqueous phase [21]. Biological wastewater treatments (secondary treatments), such as the use of activated sludge and membrane bioreactors, are also not effective for CBZ removal due to its resistance to biodegradation [18].

In order to enhance the removal of CBZ in WWTPs, several advanced technologies have been tested as tertiary treatments, but so far none has appeared as an adequate solution [18]. For instance, CBZ removal by reverse osmosis and nanofiltration membranes is above 90% [22,23]; however, these methods also present limitations such as membrane fouling and high operation costs associated with the high pressures used in the process [24]. Another approach is the use of advanced oxidation processes, such as ozonation [25], UV/H₂O₂ [26], UV/TiO₂ [27], and Fenton processes [28], which are effective for CBZ removal. However, the costs associated with the addition of chemicals, the separation of catalysts [18], and sludge management, as well as the possibility of generating toxic byproducts, need to be considered. Adsorption, another treatment option, is one of the most promising due to its efficiency, simple design, and low cost. Furthermore, it does not lead to the formation of toxic intermediate compounds [29]. One of the most crucial factors in this process is the adsorption capacity of the used material [29], and therefore, activated commercial carbon is commonly used because of its high adsorption capacity. The use of granular and powdered activated carbon provides efficient CBZ removal, ranging from 90 to 99% [30,31]. Nevertheless, it is necessary to overcome the restrictions associated with the high price of activated carbon and the limitations associated with its regeneration [32]. Recently, biochars (waste biomass pyrolysis products) have drawn attention as alternative adsorbents to activated carbon due to their physicochemical properties and widespread availability [33]. Besides adsorption, electrochemical processes have gained increasing interest in recent years to treat polluted waters, and were applied by Alighardashi et al. [34] to remove CBZ from wastewaters. Electrochemical systems offer several advantages, such as simple operation (at ambient temperature and pressure), robust performance, the capability to adjust to variations in the influent composition and flow rate [35], and viability in degrading nonbiodegradable pollutants [36]. In contrast with the conventional two-dimensional (2D) process, in which there are only two electrodes (cathode and anode), in a three-dimensional (3D) process, a third electrode can be utilized. If this electrode is composed of particles, an extraordinarily expansion of its specific surface area is achieved. Under an electric field, these particles with specific shapes and sizes can be polarized,

mimicking charged microelectrodes and delivering higher electrocatalytic efficiency [37]. The removal of pollutants in 3D systems is 10–50% higher than in 2D systems, while simultaneously reducing energy consumption [35]. Alighardashi et al. [34] applied a 3D electrochemical process for CBZ degradation employing two aluminum electrodes, as both anode and cathode, and powdered activated carbon as the particulate electrode, achieving a removal efficiency of 89.8%.

In this context, the aim of the present work was to apply a 3D electrochemical process to the degradation of CBZ, considering the influence of the anode and cathode materials, type of carbon-based adsorbent (biochar and commercial activated carbon), and other operational parameters, such as current density, reaction time, electrolyte concentration, distance between the electrodes, and CBZ concentration.

The use of biochar may prove to be a key and accessible input for sustainability, as it has many potential socio-economic and environmental benefits in the framework of the circular economy.

2. Materials and Methods

2.1. Reagents and Materials

CBZ was purchased from Sigma-Aldrich (St. Louis, MI, USA). Acetonitrile HPLC-grade (Carlo Erba, Barcelona, Spain) was used as the organic eluent in the high-performance liquid chromatographic (HPLC) method. Sodium chloride was obtained from Fisher Scientific (Hampton, NH, USA), formic acid 98–100% was acquired from VWR (Alfragide, Portugal), hydrochloric acid 37% p.a. was obtained from Scharlau (Barcelona, Spain), and sodium hydroxide was purchased from Merck (Darmstadt, Germany). A stock solution of CBZ (1000 mg/L) was prepared in acetonitrile and stored at $-10\text{ }^{\circ}\text{C}$. The working solutions were prepared daily by diluting the stock solution with ultrapure water before use. Ultrapure water (18.2 M Ω .cm resistivity) was obtained using a purification system from Millipore (Molsheim, France). The CBZ working solution had an initial pH of 5.

A boron-doped diamond (BDD) electrode (DIACHEM[®] electrode type, 100 × 20 × 2 mm, niobium substrate, both sides coated, multilayer—from CONDIAS, Itzehoe, Germany) and a mixed metal oxide (MMO) electrode (titanium-coated with RuO₂-IrO₂-TiO₂, 10.50 μm thickness, 100 × 20 × 2 mm, UTronTechnology, Youchuang, China) were used as the anode, and stainless steel (STS) (AISI-304, austenitic grade, 100 × 20 × 2 mm) was used as the cathode in the 2D and 3D electrochemical experiments. An HQ Power, adjustable DC power supply, model PS3020 (Velleman[®], Gavere, Belgium) with an adjustable output voltage of 0–30 V and an adjustable output current of 0–20 A was used to carry out the electrochemical processes.

Vineyard pruning residues from Touriga Nacional (TN), gently provided by Sogrape Vinhos, S.A. (Porto, Portugal), sampled at Quinta dos Carvalhais (Dão wine region) in 2015, were used to produce the biochar. The vineyard pruning residues were pyrolyzed in an industrial oven by Ibero Massa Florestal (Aveiro, Portugal), as previously described by Fernandes et al. [38]. Briefly, the biomass was pyrolysed (without any nitrogen or carbon dioxide supply): 8 h of heating time, 14 h of holding at 500 $^{\circ}\text{C}$, and cooling for 18 h until room temperature. The obtained biochar was milled (ZM200, Retsch, Haan, Germany) and sieved (AS 200 Basic Retsch, Haan, Germany) to obtain two fractions with particle sizes of 1–2 mm and <75 μm that were used in the experiments. The moisture and ash contents of the biochars were determined following the ASTM D1762 standard.

One polymer-based spherical activated carbon (PBSAC) was supplied by SARATECH[®] reference 102282 (Blücher, Erkrath, Germany).

2.2. Conductivity and pH Measurement

Conductivity and pH measurements were performed using a multiparameter analyzer Consort C861 (Turnhout, Belgium) equipped with a conductivity electrode (Consort SK10B) and a pH electrode (Consort SP10B).

2.3. Quantification of CBZ

CBZ analysis was performed using a Shimadzu HPLC equipment (Shimadzu Corporation, Kyoto, Japan) equipped with an LC-20AB pump, a DGU-20A5 degasser, a SIL-20A automatic injector, a CTO-20AC column oven, and an SPD-M20A diode-array detector. The separation was performed with a LUNA C18 column (particle size 5 μm , 150 \times 4.60 mm), using a C18 precolumn (particle size 5 μm , 4 \times 2.0 mm), both from Phenomenex (Torrance, CA, USA). Ultrapure water with 0.1% formic acid (A) and acetonitrile (B) were used as eluents. The chromatographic program is described in Table 1. The control of the chromatographic system and the acquisition and processing of chromatographic data were made using LC solution version 1.25 SP2 software. CBZ quantification was carried out using external calibration. For that, different solutions with concentrations ranging from 2.5 to 20,000 $\mu\text{g/L}$ were prepared in water from the respective stock solution. The concentration of CBZ assessed in each sample, resulting from triplicate injections, was expressed as mg/L.

Table 1. Chromatographic conditions for CBZ analysis.

Time (min)	% Acetonitrile (B)	Oven Temperature ($^{\circ}\text{C}$)	Injection Volume (μL)	Flow Rate (mL/min)	Wavelength (nm)
0	10				
7	80				
10	10	35	20	1.0	285
14	10				

2.4. 2D Electrochemical Process

The two-dimensional (2D) electrochemical process for the removal of CBZ was carried out in a single-compartment electrochemical cell, working in batch-operation mode. An acrylic reactor (2 \times 15 \times 8 cm) was built with a rectangular base with a total volume capacity of 240 mL (Cromotema, Vila Nova de Gaia, Portugal), with the possibility of placing the electrodes at two different distances, 3.5 and 7.5 cm. All electrodes used (BDD, MMO, and STS) had a submerged area of 15 cm^2 . An aqueous CBZ solution (150 mL), containing NaCl as electrolyte, was transferred to the electrochemical cell while maintaining an airflow of 3000 cm^3/min during the process (selected after preliminary studies). An ELITE 802 air pump with 2 outputs of 1500 cm^3/min each (Hagen, Yorkshire, United Kingdom) was used as the air supplier. The current intensity was maintained constant at 0.1, 0.2, and 0.3 A, corresponding to a current density of 6.67, 13.3, and 20 mA/cm^2 , respectively. Besides different current densities, the operational conditions were optimized considering the pH, CBZ and NaCl concentrations, reaction time, distance between electrodes, and anode material (BDD and MMO). Aliquots of CBZ solution (1000 μL each) were taken at regular periods during the experiments, and the evolution of the CBZ removal was assessed by HPLC. All experiments were performed in triplicate.

2.5. CBZ Adsorption Experiments

Preliminary studies, adsorption kinetic and equilibrium studies, as well as pH influence experiments, were carried out in Erlenmeyer flasks; the solution was magnetically stirred at 370 rpm (Multistirrer 15, Velp Scientifica) at room temperature (21 $^{\circ}\text{C}$). Different amounts of the PBSAC and biochars were weighed using an analytical balance (Mettler Toledo, model MS205DU1, Columbus, OH, USA) and added to Erlenmeyer flasks containing 25 mL of CBZ solution at various initial concentrations (2.5 mg/L to 10 mg/L), with pH values ranging from 3 to 9. For kinetic, equilibrium, and pH studies, the initial CBZ concentration was 10 mg/L. At the end of the assays, an aliquot of the final solutions was immediately centrifuged (Heraeus Fresco 21 Microcentrifuge, Thermo Scientific, Waltham, MA, USA) at 14,500 rpm for 10 min at 4 $^{\circ}\text{C}$. Then, the supernatant was vacuum-filtered through nylon membrane filters with a 0.22 μm pore size (Filter-Lab[®], Barcelona, Spain)

and analyzed by HPLC to determine the final concentration. In parallel, blank assays were prepared with the same CBZ concentration without adsorbent. The assays were performed in triplicate, and the results were expressed as mean and standard deviation (SD).

2.6. 3D Electrochemical Process

The best conditions for CBZ removal, assessed from the 2D electrochemical process and the adsorption experiments, were applied to perform the 3D electrochemical process. First, 0.150 g of the carbon materials was placed in the electrochemical cell between the anode and the cathode. Aliquots (1000 μL) were taken at constant periods, and each aliquot was filtered using a nylon microfilter (0.22 μm pore size) before HPLC analysis. All experiments were performed in triplicate.

2.7. Data Analysis

2.7.1. Modeling of Kinetic and Equilibrium Adsorption Studies

The following models were applied to fit the data by nonlinear curve fitting using Origin software (Origin Lab Corporation, Northampton, MA, USA).

The adsorption capacity (q) was determined as:

$$q = (C_0 - C_t) \times \frac{V}{m} \quad (1)$$

where C_0 and C_t (mg/L) are the initial and instant t CBZ concentrations, respectively; V is the solution volume (L); and m (g) is the adsorbent mass.

The pseudo-first-order kinetic model [39] is given by Equation (2):

$$q_t = q_e \left(1 - e^{-k_1 t}\right) \quad (2)$$

where t is time, q_t is the adsorption capacity at time t , q_e is the equilibrium adsorption capacity, and k_1 is the pseudo-first-order rate constant.

The pseudo-second-order kinetic model [40] is given by Equation (3):

$$q_t = \frac{q_e^2 k_2 t}{1 + q_e k_2 t} \quad (3)$$

where k_2 is the pseudo-second-order rate constant.

Langmuir (1918) [41] and Freundlich (1907) [42] (Equations (4) and (5)) models were applied to the study of adsorption equilibrium.

$$q_e = \frac{q_m k_L c_e}{1 + k_L c_e} \quad (4)$$

where C_e is the equilibrium concentration of the adsorbate (mg/L), q_e is the adsorption capacity at equilibrium (mg/g), K_L is the Langmuir equilibrium constant related to the energy of adsorption (L/mg), and q_m is the maximum adsorption capacity (mg/g), which in this model should correspond to a monolayer coverage of the adsorbent surface.

$$q_e = k_F (c_e)^{\frac{1}{n_F}} \quad (5)$$

where K_F is the Freundlich isotherm constant ((mg/g) (L/mg) $^{1/n_F}$), and n_F (dimensionless) is the Freundlich exponent that describes the strength of adsorption. Typically, the $1/n_F$ value ranges between 0 and 1, and if $1/n_F$ is closer to 0, the adsorption intensity is higher.

2.7.2. Electrochemical Treatment Processes

Statistical Analysis

Statistical analyses were performed with IBMS SPSS for Windows, version 26 (IBM Corp., Armonk, NY, USA). The data normality was assessed by Kolmogorov–Smirnov, and Shapiro–Wilk tests, and by visual inspection of histograms. Removal in % was represented as mean \pm standard deviation. For each 3D treatment, comparisons between groups were made using the Mann-Whitney test, at a level of significance of $p < 0.05$.

Parameters

For all tests performed, the percentage of CBZ removal was calculated using Equation (6) [24]:

$$\text{Removal (\%)} = \frac{C_0 - C_t}{C_0} \times 100 \quad (6)$$

where C_0 and C_t correspond to the initial and final concentrations of CBZ (mg/L), and t is the time, which varied between 1 and 60 min, depending on the experiments.

With the results obtained, the energy consumption (E_{Con}) associated with each of the tests was calculated, using Equation (7) [43] and the current efficiency (CE_f) applied, using Equation (8) [44]:

$$E_{Con}(\text{Wh/g}) = \frac{U I \Delta t}{(C_0 - C_t) V} \quad (7)$$

where U is the potential difference (V), I is the current intensity (A), t is the contact time (h), V is the treated volume (L), and C_0 and C_t are the initial and instant t concentrations of CBZ (g/L).

$$CE_f(\%) = FV \frac{C_0 - C_t}{I t} \times 100 \quad (8)$$

where F is the Faraday constant (96,500 C/mol), V is the treated volume (L), I is the current intensity (A), t is the processing time (s), and C_0 and C_t are the initial and instant t concentrations of CBZ (mol/L).

If target contaminants are present at low concentrations, a more appropriate parameter for estimating the energy efficiency of the electrochemical treatment may be the electric energy per order (EEO) [43]. EEO is a criterion that expresses the electric energy (in kWh/m³) required to reduce the concentration of CBZ by one order of magnitude in a unit volume of contaminated water, which is calculated by Equation (9):

$$EEO(\text{kWh/m}^3) = \frac{Pt1000}{V \log\left(\frac{C_0}{C_t}\right)} \quad (9)$$

where P is the rated power of the system (kW), V is the volume of solution treated (L) at time t (h), and C_0 and C_t are the initial and at instant t concentrations of CBZ (mol/L).

Two kinetic models, the first-order model (Equation (10)) and the second-order model (Equation (11)), were used to adjust the experimental results of CBZ degradation:

$$\ln \frac{C_0}{C_t} = k_1 \cdot t \quad (10)$$

$$\frac{1}{C_t} - \frac{1}{C_0} = k_2 \cdot t \quad (11)$$

In these equations, C_0 and C_t are the initial CBZ concentration and the concentration at time t (s) (mol/L), respectively; k_1 (s⁻¹) is the first-order rate constant; and k_2 (L/(mol·s)) is the second-order rate constant.

3. Results and Discussion

3.1. 2D Electrochemical Process Operational Conditions

3.1.1. Effect of Anode Material on CBZ Removal

Considering that the most important characteristics of the electrodes used in an electrochemical system are their stability, long service life, and electrocatalytic properties, and that the anode mainly controls the current efficiency, selectivity, and catalytic activity of the system [35], the influence of different anodes (BDD and MMO) on the CBZ removal was evaluated, using the same material (STS) as the cathode (Figure 1).

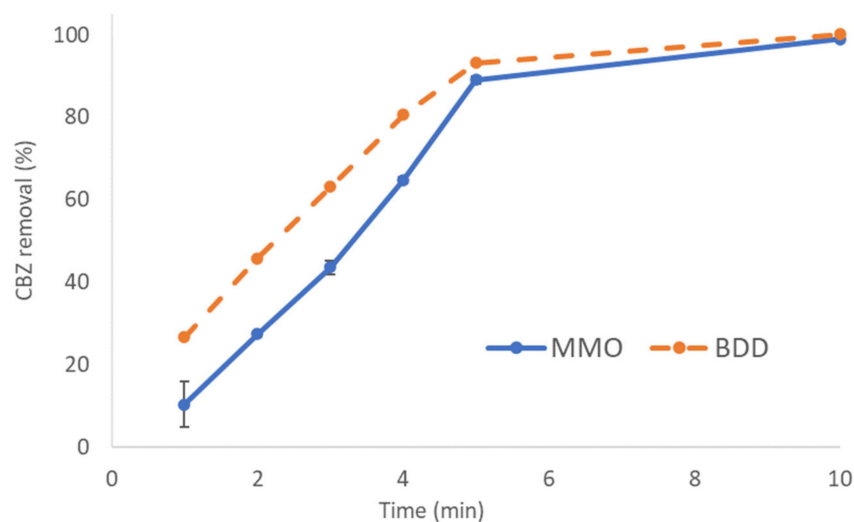


Figure 1. Effect of the anode material on CBZ removal in aqueous solutions (operational conditions: current density = 6.67 mA/cm²; inter-electrode distance = 3.5 cm; NaCl = 0.1 M; CBZ_i = 10 mg/L; pH = 5; reaction time = 10 min; cathode = STS).

The results obtained showed that the BDD anode presented a slightly better performance during the first 5 min of the electrolysis, removing 63% of CBZ after 3 min and 93% after 5 min. For the MMO anode, 44% of CBZ was removed after 3 min, and 89% after 5 min. The removal efficiency for both anodes was very similar after 5 min, reaching 100% at 10 min.

For the removal of pharmaceuticals from water, Ti-based anodes are the most widely used, as they have extended lifetimes and significant electrocatalytic activities, and are less expensive when compared to BDD [35].

For these reasons, and considering the results obtained, the MMO anode was chosen to perform the subsequent electrochemical experiments using the STS electrode as the cathode.

3.1.2. Effect of Interelectrode Distance, Reaction Time, and Current Density on CBZ Removal

To assess the effect of interelectrode distance on CBZ removal, two different distances were tested (3.5 and 7.5 cm). It can be seen in Figure 2 that 3.5 cm resulted in a higher CBZ removal rate. When the interelectrode distance was 7.5 cm, the CBZ removal was 80% after 45 min, while at $d = 3.5$ cm, CBZ was completely removed after 10 min. This might be due to the short distance, which favored the mass transfer [45]. Thus, an interelectrode distance of 3.5 cm was chosen to continue the work.

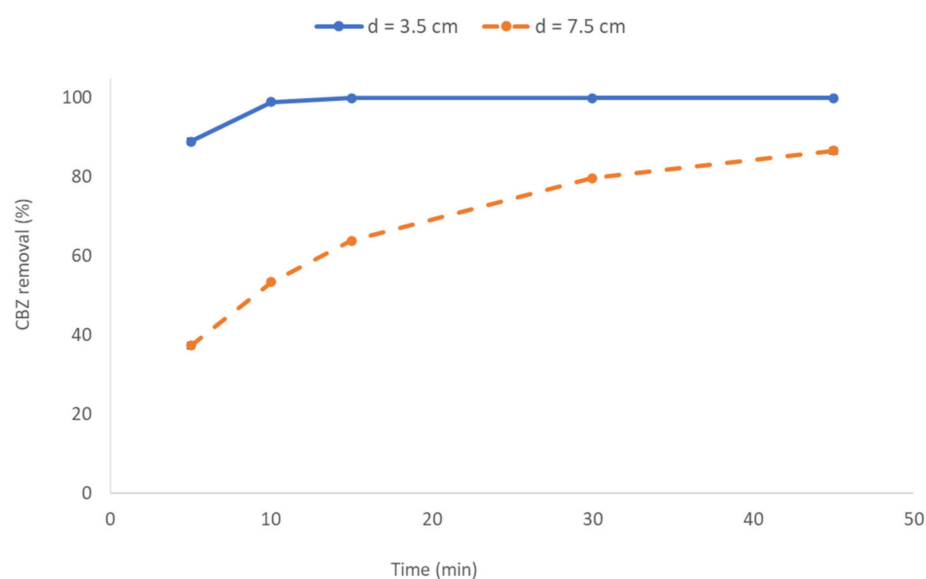


Figure 2. Effect of interelectrode distance on the removal of CBZ from aqueous solutions (operational conditions: $j = 6.67 \text{ mA/cm}^2$; $\text{NaCl} = 0.1 \text{ M}$; $\text{CBZi} = 10 \text{ mg/L}$; $\text{pH} = 5$; reaction time = 45 min; cathode = STS; anode = MMO).

The effect of the reaction time on CBZ removal can be analyzed using Figure 2. With the increase of the reaction time, the production of strong oxidizing substances in the reactor rose, causing an increase in the CBZ removal rate [45]. However, an increase of the reaction time corresponded to an increase of the hydraulic retention time in continuous operation, and consequently larger reactors and higher energy consumption. Therefore, it was most appropriate to select the minimum reaction time that allowed a high removal efficiency, which was 10 min for 100% removal in the studied system.

As stated by Lin et al. [46], current density (j) is an important parameter that can be directly controlled during the electrochemical oxidation process. Therefore, different j values were tested, placing the anode and cathode at different distances, and the results (Table 2) showed that an increase in j had a positive impact on the removal of CBZ. A higher current density resulted in a higher cell potential, and consequently a higher energy consumption for the same reaction time (10 min). Considering the degradation efficiency and energy consumption, using a 3.5 cm interelectrode distance, the optimum j for the 2D process should be 6.67 mA/cm^2 . These results also highlighted the fact that an increase in potential does not translate into greater efficiency removals.

Table 2. Current density, interelectrode distance, CBZ removal (%), potential, and energy consumption for the 2D electrochemical removal of CBZ from aqueous solutions using an MMO anode and an STS cathode.

j (mA/cm^2)	Interelectrode Distance (cm)	CBZ Removal (%)	Potential (V)	ECon (Wh/g)
6.67	3.5	96.4	5.40	68.7
	7.5	80.2	8.20	118
13.30	3.5	99.3	7.70	91.2
	7.5	99.1	16.5	193
26.70	3.5	99.9	13.6	158
	7.5	99.2	25.8	301

Operational conditions: $\text{NaCl} = 0.1 \text{ M}$; conductivity = $13.6 \pm 0.2 \text{ mS/cm}$; $\text{CBZi} = 10 \text{ mg/L}$.

3.1.3. Effect of Electrolyte Concentration on CBZ Removal

The influence of the electrolyte (NaCl) concentration (0.01 M and 0.1 M) on the CBZ removal was studied. The results presented in Figure 3 showed that the higher NaCl concentration (0.1 M) provided a faster removal of CBZ. This was due to the increase in conductivity of the solution. A low electrolyte concentration results in a poor conductivity of the solution and the inability to produce sufficiently strong oxidizing substances [45]. Besides this, if NaCl is used as electrolyte, Ti-based anodes generate chlorine species (Cl_2 , HOCl, and ClO^-), which help the degradation of organic material by indirect and direct oxidation [34]. Therefore, 0.1 M was selected as the optimum electrolyte concentration.

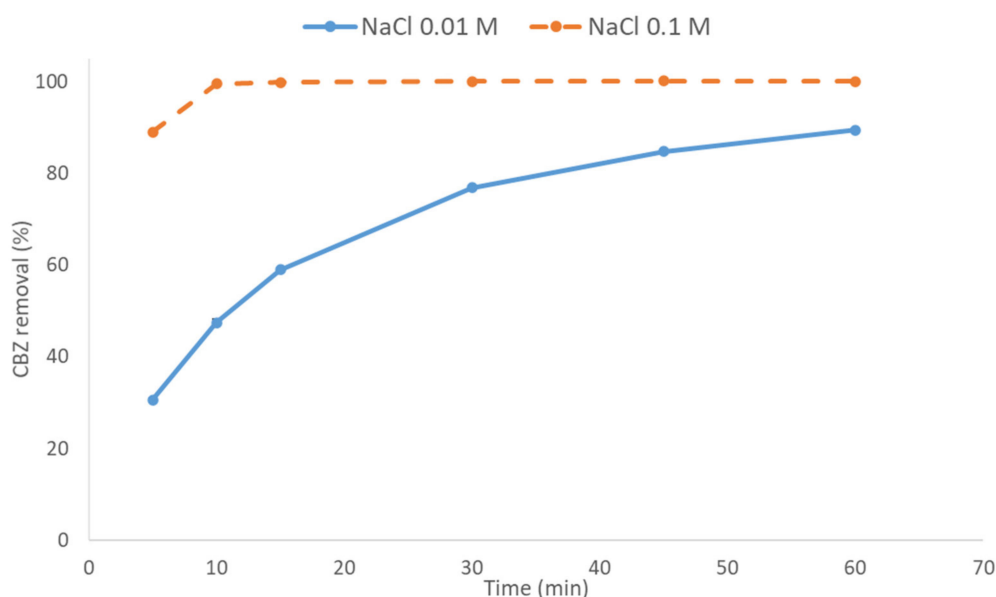


Figure 3. Effect of NaCl concentration on the removal of CBZ from aqueous solutions (operational conditions: $j = 6.67 \text{ mA/cm}^2$; interelectrode distance = 3.5 cm; $\text{CBZ}_i = 10 \text{ mg/L}$; pH = 5; reaction time = 60 min; cathode = STS; anode = MMO).

3.1.4. Effect of pH on CBZ Removal

The influence of the initial pH on the CBZ removal was studied for different pH values: 3, 5, 7, and 9. The pH value was adjusted with HCl and NaOH solutions. The CBZ working solution had a pH of 5. The results shown in Figure 4 indicated that the CBZ removal was much faster at pH 3 than that for the other studied pH values. Nevertheless, for these pH values, the removal rate was very similar, around 90% after 5 min.

These results were in accordance with those obtained by Yang et al. [47], who studied the effect of pH on the removal of CBZ in a photocatalytic process and found that at low pH values, the degradation of CBZ was higher than that observed at pH values close to neutrality. The authors hypothesized that the CBZ CONH_2 group was more susceptible to degradation at acidic pH.

Considering the typical pH range of domestic wastewater (around 7,) the use of pH 3 would imply a pH adjustment, which would increase the operational costs and would not be adequate for the discharge of the effluents in the aquatic environment. Therefore, pH 7 was considered the best choice for the remaining experiments. The low sensitivity of CBZ removal to the variation of pH in the range between 3 and 9 could be explained by its presence in the neutral form in this pH range, as shown in Figure 5.

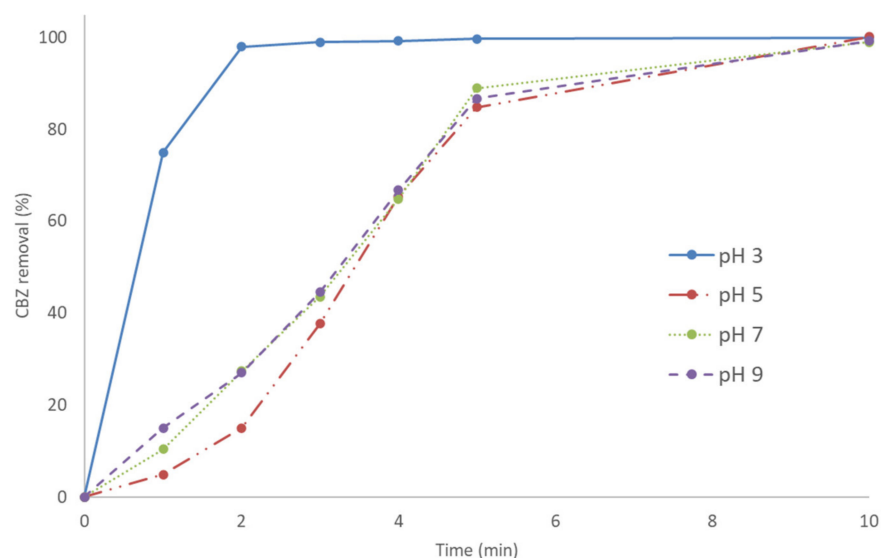


Figure 4. Effect of pH on the removal of CBZ from aqueous solutions (operational conditions: $j = 6.67 \text{ mA/cm}^2$; distance = 3.5 cm; NaCl = 0.1 M; CBZi = 10 mg/L; reaction time = 10 min; cathode = STS; anode = MMO).

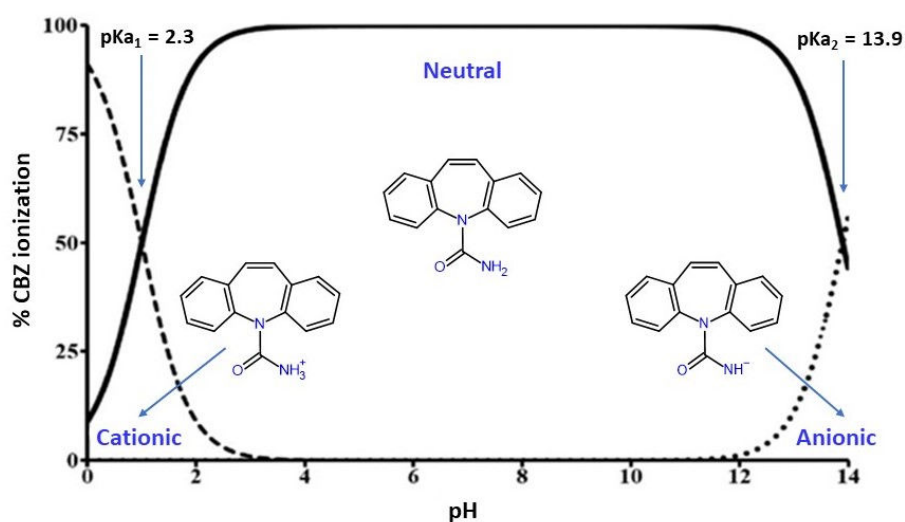


Figure 5. Speciation of CBZ as a function of the pH of the aqueous solution (adapted from [48]).

The spectral analysis confirmed that even after 60 min of solution preparation, there was no evidence of CBZ spectrum changes (changes in the chemical species) in the pH range studied that could interfere in the CBZ quantification and consequently in the degradation observed in the electrochemical experiments (Supplementary Figure S1).

3.1.5. Effect of Initial CBZ Concentration on CBZ Removal

The influence of the initial CBZ concentration, ranging from 2.5 to 10 mg/L, on its removal was studied. Figure 6 shows that the degradation efficiency of CBZ decreased as the initial CBZ concentration increased. This may be attributed to the presence of refractory functional groups, such as the benzene ring, which may inhibit the catalytic reaction [45]. Although the degradation was much faster at lower concentrations, the initial concentration of 10 mg/L, used previously, was considered adequate for the following experiments, because this was the least favorable situation, and at the same time allowed the evaluation of the influence of the process variables within a wider range.

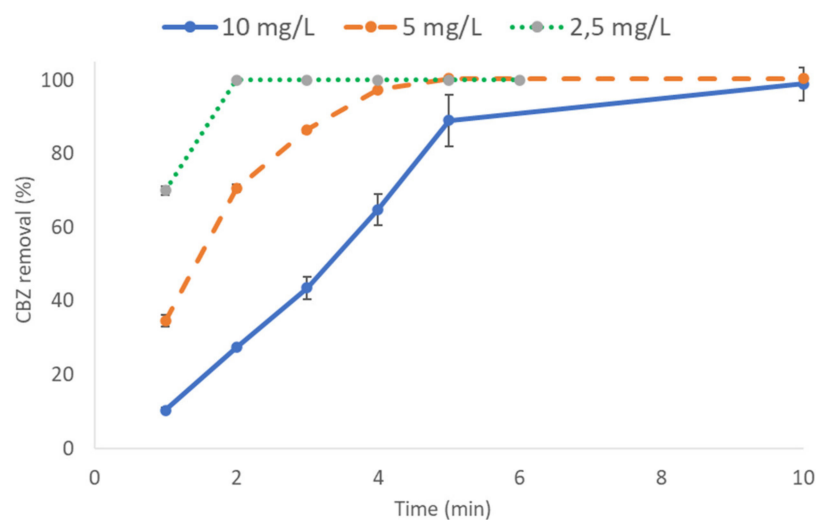


Figure 6. Effect of the initial CBZ concentration on CBZ removal from aqueous solutions (operational conditions: $j = 6.67 \text{ mA/cm}^2$; $\text{NaCl} = 0.1 \text{ M}$; $\text{pH} = 7$; reaction time = 10 min; cathode = STS; anode = MMO).

Based on the results of these studies, we concluded that the optimum conditions for the removal of CBZ using the 2D electrochemical process were: current density = 6.67 mA/cm^2 , electrolyte (NaCl) concentration = 0.1 M , $\text{pH} = 7$, interelectrode distance = 3.5 cm , reaction time = 10 min, and initial CBZ concentration = 10 mg/L , using MMO as the anode and STS as the cathode. Under these conditions, the removal rate of CBZ was up to 95%.

3.2. Adsorption Experiments

3.2.1. Characterization of the Adsorbents

Table 3 summarizes the characteristics of the adsorbents. The particle size was especially important because it influenced the adsorptive capacity of the adsorbents. The biochar of TN with $<75 \mu\text{m}$ had the smallest particle size, but SARATECH[®] had the highest surface area. The biochars presented a higher ash and moisture content than the SARATECH[®] activated carbon.

Table 3. Characteristics of the adsorbents.

			
Parameters	SARATECH [®] -102282	Biochar TN	Biochar TN
Ash content (%)	0.2	5.90	5.90
Moisture content (%)	0.1	4.32	4.32
Particle size (mm)	0.457	<0.075	1.0–2.0
Surface area (m^2/g) BET	1736	62	62

3.2.2. Kinetic Studies and Isotherms

The results concerning kinetic behavior (Table 4) revealed that the adsorption of CBZ onto the biochars was better described by a pseudo-first-order reaction (it was not possible to adjust the pseudo-second-order model to kinetic results of the biochar TN $<75 \mu\text{m}$). An analysis of the k_1 values (Table 4) showed that the k_1 value for the CBZ/biochar TN $<75 \mu\text{m}$ was higher than that for biochar 1–2 mm. Thus, the adsorption rate of CBZ on

the smaller biochar was faster than for 1–2 mm. The activated carbon from SARATECH® showed almost instant adsorption of CBZ, therefore it was not possible to adjust the results to kinetic models.

Table 4. Parameters for the kinetic and isotherm studies.

Kinetic Models		
Adsorbents	Pseudo first order	Pseudo second order
SARATECH®	–	–
Biochar < 75 µm	R ² = 0.998 q _e = 0.769 mg/g k ₁ = 1388 min ⁻¹	–
Biochar 1–2 mm	R ² = 0.916 q _e = 0.137 mg/g k ₁ = 0.119 min ⁻¹	R ² = 0.908 q _e = 0.153 mg/g k ₂ = 1.00 g/mg·min
Equilibrium Models		
Adsorbents	Langmuir	Freundlich
SARATECH®	R ² = 0.849 q _m = 7.95 mg/g K _L = 2.66 L/mg	R ² = 0.976 K _F = 4.97 (mg/g)·(L/mg) ^{1/n} n _F = 3.66
Biochar < 75 µm	R ² = 0.945 q _m = 1.12 mg/g K _L = 0.643 L/mg	R ² = 0.988 K _F = 0.495 (mg/g)·(L/mg) ^{1/n} n _F = 3.03
Biochar 1–2 mm	R ² = 0.981 q _m = 0.754 mg/g K _L = 1.06 L/mg	R ² = 0.992 K _F = 0.503 (mg/g)·(L/mg) ^{1/n} n _F = 3.19

The equilibrium adsorption isotherm is fundamental to describe the interactive behavior between solutes and adsorbents, and is the basic requirement in the design of adsorption systems [49].

The calculated constants for the Freundlich and Langmuir equilibrium models are presented in Table 4. These isotherms showed a characteristic L-type behavior according to the Giles classification, thus representing a system in which the adsorbate was strongly attracted by the adsorbent [49]. Although all models described the experimental results well, taking into consideration the parameters obtained, the Freundlich equation gave a better representation of the experimental results for all the tested adsorbents.

Considering the adsorption capacity, the SARATECH® and the biochar TN < 75 µm were chosen for further optimization studies.

3.2.3. Effects of Different Parameters on CBZ Adsorption

Influence of pH

The effect of four different pH values (3, 5, 7, and 9) on the adsorption of CBZ onto the biochar TN < 75 µm and SARATECH® was investigated (Figure 7). The highest adsorption capacity for the biochar was obtained at pH 5, while for SARATECH®, the maximum was observed at pH 9. For the SARATECH®, there was an increase in the adsorption capacity from pH 5 to 9. This increase was less pronounced between pH 7 and 9.

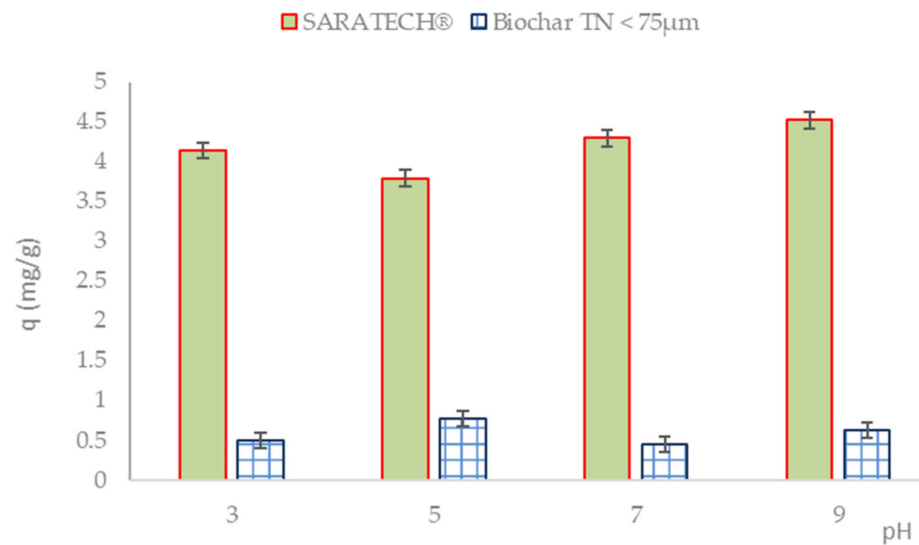


Figure 7. Effect of pH on adsorption capacity.

In general, the variation of the pH of the solution may affect the functional groups of both the pharmaceutical and the adsorbent; however, in the pH range studied, only the adsorbent might be influenced. CBZ is a neutral compound in the entire studied pH range, and its adsorption behavior is different from ionized compounds, which can be affected by electrostatic forces. One should also take into consideration a phenomenon affecting both neutral and ionizable compounds that consists of the size exclusion of large sorbate molecules from microporous carbonaceous sorbents. The NH_2 functional group in CBZ can interact with oxygen-containing functional groups of the adsorbents, such as OH and CO, through hydrogen bonding [33,50].

At lower pH values, functional groups on adsorbents and CBZ can interact with H^+ more easily due to their abundance in the solution, which decreases hydrogen bonding between the adsorbents and CBZ, and consequently decreases adsorption efficiency [33]. In contrast, as the concentration of H^+ is reduced at higher pH levels, hydrogen-bonding donor groups on CBZ can interact with hydrogen-bonding acceptors or donors in the adsorbents, and therefore the adsorption efficiency is expected to be enhanced [33].

For the 3D experiments, pH 7 was chosen after considering the common pH of domestic wastewaters and the obtained results in the optimization of adsorption and 2D studies.

Influence of Initial CBZ Concentration

The adsorption capacity increased with increasing CBZ concentration for the SARATECH® activated carbon (Figure 8), which indicated that there still were active adsorption sites available for a 10 mg/L solution. However, it is expected that further increases in CBZ concentration could result in a plateau of adsorption capacity and a decline of adsorption efficiency, because there are no longer available sites for adsorption. For the biochar TN < 75 µm, no significant differences were observed for the different concentrations (Figure 8), which may be related to its low specific surface area and consequently lower availability of active adsorption sites.

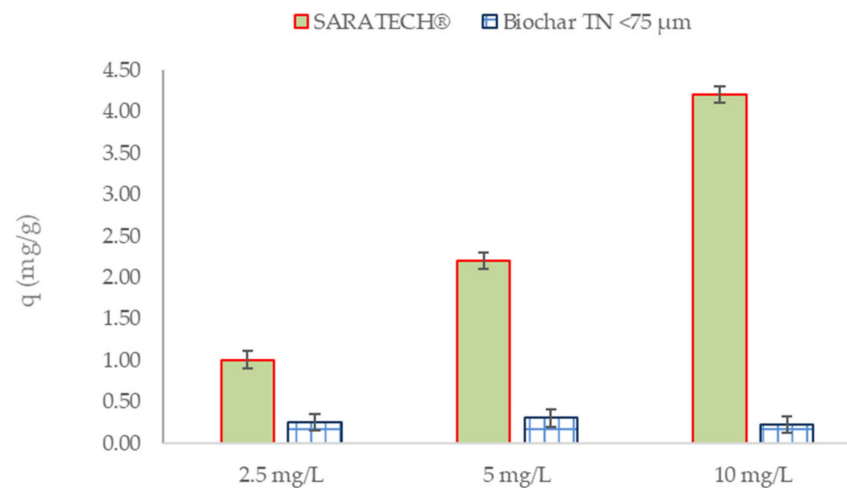


Figure 8. Effect of initial CBZ concentration on the adsorption capacity of Biochar TN < 75 μm and the activated carbon from SARATECH®.

Influence of Electrolyte

Considering that the addition of an electrolyte is mandatory in 2D and 3D electrochemical treatments, the influence of the use of a 0.1 M NaCl solution (at pH 7) on the adsorption capacity (Figure 9) was also tested. No significant changes were observed for the SARATECH® activated carbon, and an increase in the adsorption capacity was observed for the biochar TN < 75 μm.

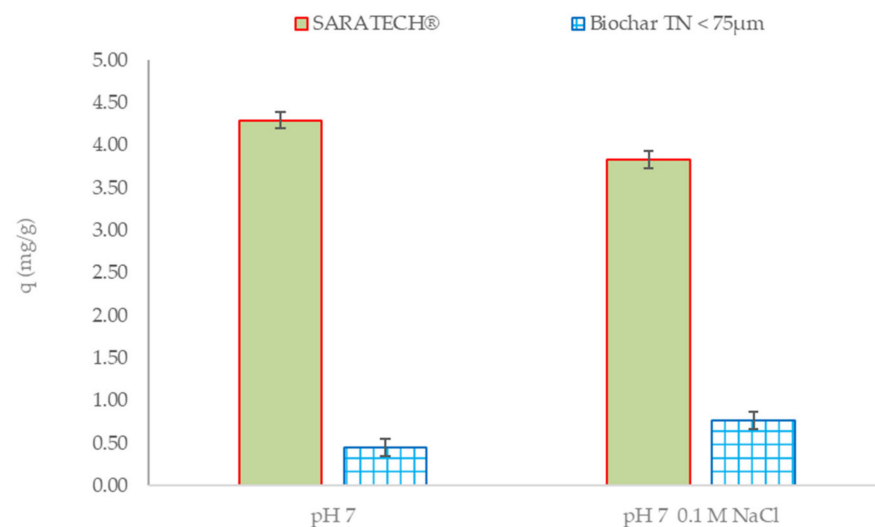


Figure 9. Effect of the electrolyte (0.1 M NaCl) on adsorption capacity.

3.3. 3D Experiments

After studying the 2D electrochemical and adsorption processes, their combination was also explored through the study of the 3D electrochemical process, for which the influences of some parameters were evaluated: interelectrode distance, particulate electrode, reaction time, energy consumption, current, and energy efficiencies.

3.3.1. Effect of Interelectrode Distance on CBZ Removal

It can be seen in Figure 10 that for a greater distance between the electrodes, the degradation efficiency of CBZ was lower in the first 10 min, 61 and 69%, respectively, for 7.5 and 3.5 cm. This can be explained by the fact that a change of the distance between electrodes affects mass transfer, electron transport, and electrical resistance [51]. After

15 min, the difference between the removal rates was less than 5%, and after 45 min there was no difference. It was also observed that the particulate electrode was dispersed in the entire reactor (Figure 11) for the shorter distance, but for the larger distance, the particulates were confined between the cathode and the anode. Therefore, an interelectrode distance of 7.5 cm was chosen to perform the 3D experiments.

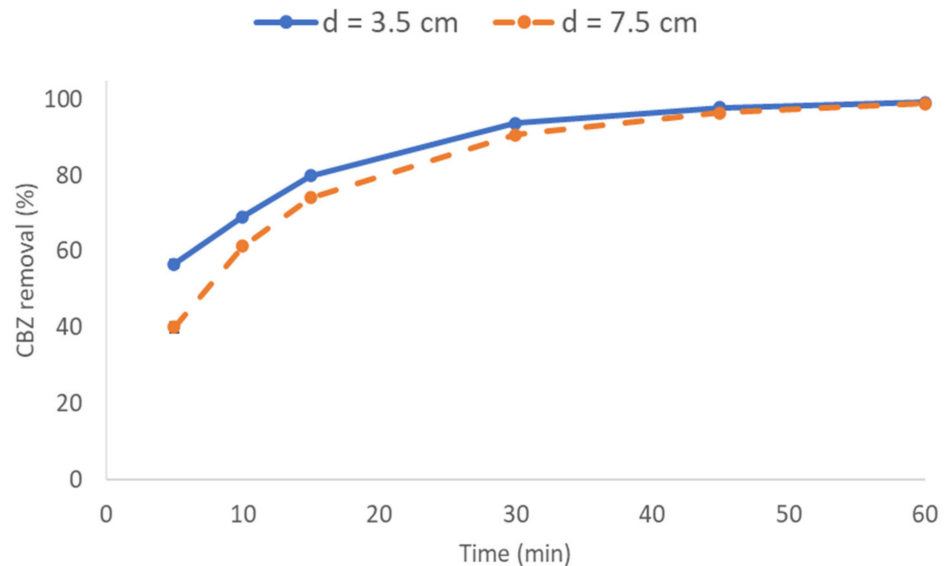


Figure 10. Effect of interelectrode distance on the CBZ removal from aqueous solutions (operational conditions: $j = 6.67 \text{ mA/cm}^2$; $\text{NaCl} = 0.1 \text{ M}$; $\text{CBZ}_i = 10 \text{ mg/L}$; $\text{pH} = 7$; reaction time = 60 min; particulate electrode = biochar TN 1–2 mm, 1 mg/mL solution; cathode = STS; anode = MMO).

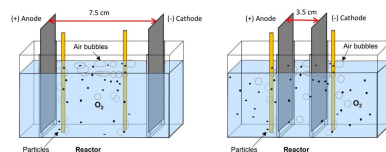


Figure 11. Schematic representations of the 3D electrochemical cell for the two tested interelectrode distances and effect on the particulate electrode distribution (biochar 1–2 mm, 1 mg/mL solution).

3.3.2. Effect of the Particulate Electrode on CBZ Removal

In a 3D particulate electrode system, the material of the particulate electrode is one of the most important factors influencing the efficiency and cost of the process [52]. In this study, the polymer-based activated carbon from SARATECH[®] and the two biochars from TN vineyard pruning residues were used as the particulate electrode.

The results of the effect of the particulate electrode on the CBZ removal efficiency are presented in Figure 12. According to the results, all the tested adsorbents led to an increase in the removal compared to the 2D process. The use of the particulate electrode allowed for an increase in CBZ removal (45 min) of 8, 14, and 15%, respectively, for biochars TN < 75 μm , TN 1–2 mm, and SARATECH[®] activated carbon when compared with the 2D process. Other studies also reported removal efficiencies that were 10 to 50% higher for 3D processes than for 2D processes [35]. The removal rate of organic pollutants, such as CBZ, improves by using the 3D electrochemical process because, besides the particulate electrode polarization, the large specific surface areas of these particles (adsorbents) can provide reactive sites for pollutant adsorption, or even catalytic reactions [51].

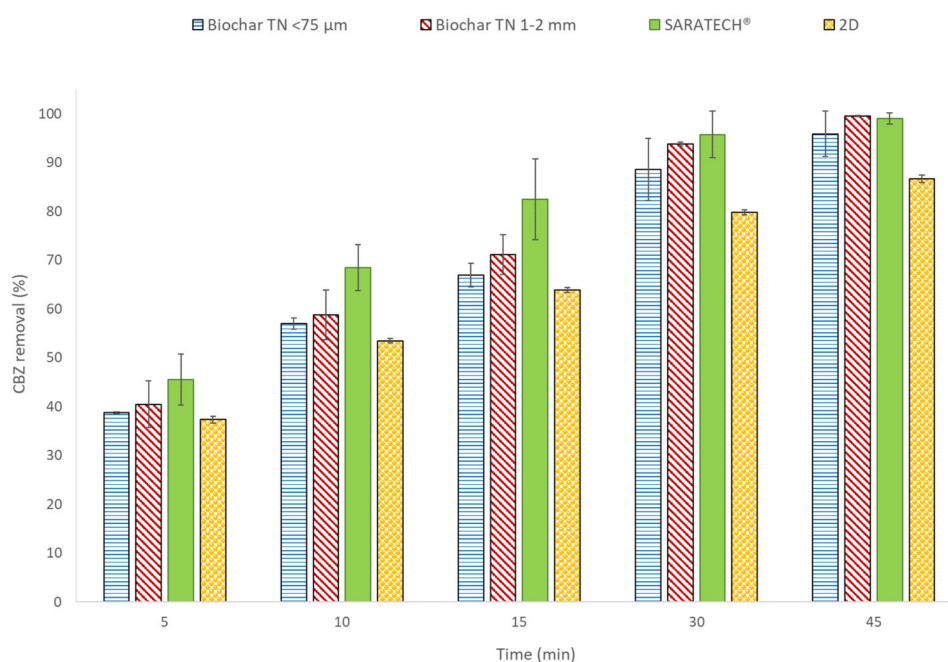


Figure 12. Effect of the particulate electrode on CBZ removal from aqueous solutions (operational conditions: $j = 6.67 \text{ mA/cm}^2$; $\text{NaCl} = 0.1 \text{ M}$; $\text{CBZi} = 10 \text{ mg/L}$; $\text{pH} = 7$; reaction time = 45 min; interelectrode distance = 7.5 cm; particulate electrode = 1 mg/mL solution; cathode = STS; anode = MMO).

The best results were obtained for the activated carbon supplied by SARATECH[®], although there were no significant differences between the three particulate electrodes at 30 and 45 min ($p < 0.05$). Activated carbon may be polarized within an electric field [53], increasing the overall active electrode area [54], which can explain the results obtained for the tested activated carbon. Nonetheless, the biochars can be a more sustainable and economic alternative to the activated carbon. Surprisingly, the biochar TN 1–2 mm, which showed a much lower adsorption capacity in the adsorption experiments, presented a removal efficiency that was very similar to the activated carbon and slightly better than the one for the biochar TN < 75 μm. It is known that the polarizability of a particulate electrode is of higher importance than its adsorption capacity [53]. In this study, it was also observed that the adsorbent with lower adsorption capacity to CBZ, when used in a 3D process, and thus after polarization, showed a completely different behavior, and very promising application perspectives.

3.3.3. Effect of the Reaction Time on CBZ Removal

The effect of the reaction time on the removal of CBZ was examined in the range of 0–45 min for the 2D and 3D electrochemical processes. As shown in Figure 12, a 30 min reaction time was needed to reach a removal efficiency of 95% in the case of the 3D process when using the biochar TN 1–2 mm and the SARATECH[®] activated carbon, after which no significant changes were observed. However, as shown in Figure 12, for the 2D process, after 30 min of reaction, the CBZ removal was only 80% (87% after 45 min).

Alighardashi et al. [34] examined the effect of the reaction time in the range of 0–60 min to remove CBZ using 2D and 3D electrochemical processes ($j = 9 \text{ mA/cm}^2$). They reported similar conclusions to this study, utilising aluminium anodes and cathodes and a powdered activated carbon particulate electrode, needing 10 min to reach a 90% removal efficiency in the case of the 3D process, which was 18 times shorter than the 2D process.

The reaction time is closely related to energy consumption and treatment performance; thus, the optimum time is when the efficiency removal is higher with minimal energy consumption. On the other hand, prolonged reaction times would increase the treatment cost [52].

In Table 5, the CBZ removal efficiency, rate constants, correlation coefficients, and half-lives are presented for the first-order and second-order kinetic models when using the 3D and 2D processes previously described.

Table 5. CBZ removal efficiency, regression coefficient, rate constant, and half-life as a function of 3D and 2D processes.

Processes		3D		2D	
Adsorbent		Biochar TN < 75 μm	Biochar TN 1–2 mm	SARATECH [®]	None
% CBZ removal		95.9	99.5	99.1	86.7
First-order model	R^2	0.9994	0.9731	0.9991	0.9835
	k_1, s^{-1}	0.00112	0.00199	0.00167	0.000635
	Half-life, min	10.5	5.8	6.8	19.3
Second-order model	R^2	0.9009	0.7298	0.8387	0.9952
	$k_2, \text{L}/(\text{mol}\cdot\text{s})$	237	2050	1045	59.5
	Half-life, min	1.8	0.2	0.4	6.7

Operational conditions: $j = 6.67 \text{ mA}/\text{cm}^2$; $\text{NaCl} = 0.1 \text{ M}$; $\text{CBZi} = 10 \text{ mg}/\text{L}$; $\text{pH} = 7$; reaction time = 45 min; interelectrode distance = 7.5 cm; particulate electrode = 1 mg/mL solution; cathode = STS; anode = MMO.

The correlation coefficients showed that for the 3D processes, the model that better described the degradation of CBZ was the first-order kinetics, while for the 2D process, it was the second-order kinetics. The results for the 2D process agreed with the work of Gurung et al. [55], who reported this model as the best to describe the degradation kinetics of CBZ when using Ti electrodes.

For the removal of CBZ, no kinetic studies were found in the literature regarding the 3D process. The correlation coefficient for the first-order model and the second-order model for the 2D process were comparable, so the first-order model also was valid for describing the reaction kinetics for this process. Comparing the first-order rate constants (k_1) for the 3D and 2D processes, the 3D process presented a higher k_1 , and the highest value was obtained when the biochar TN 1–2 mm was used; regarding the half-lives for these processes, the CBZ concentration was reduced by 50% in a shorter time when using biochar TN 1–2 mm (5.8 min) than in the other conditions.

3.3.4. Effect on Energy Consumption, Current, and Electric Efficiencies

Bolton et al. [43] proposed standard figures of merit for the comparison and evaluation of advanced oxidation technologies, based on electric energy consumption and providing a direct link to the electric efficiency (lower values meaning higher efficiency), independently of the nature of the system, and therefore allowing direct comparison of different treatments (Figure 13).

The current efficiency was higher in the 3D process (0.21% for all the particulate electrodes) in comparison with the 2D process (0.18%) (Figure 13A). The energy consumption of the 3D process (Figure 13B) was lower when using the biochar TN 1–2 mm (390 Wh/g), followed by the biochar TN < 75 μm (394 Wh/g) and SARATECH[®] activated carbon (401 Wh/g). The 2D process presented the highest energy consumption (418 Wh/g). The electric energy per order can be defined as the electric energy (kWh) required to degrade a contaminant by one order of magnitude in a unit volume (m^3) of contaminated water [43]. Figure 13C shows that the 3D process, mainly using the biochars (2237 and 2709 kWh/ m^3 for biochar TN < 75 μm and biochar TN 1–2 mm, respectively), reduced the electric energy per order (EEO) when compared with the 2D process (7507 kWh/ m^3).

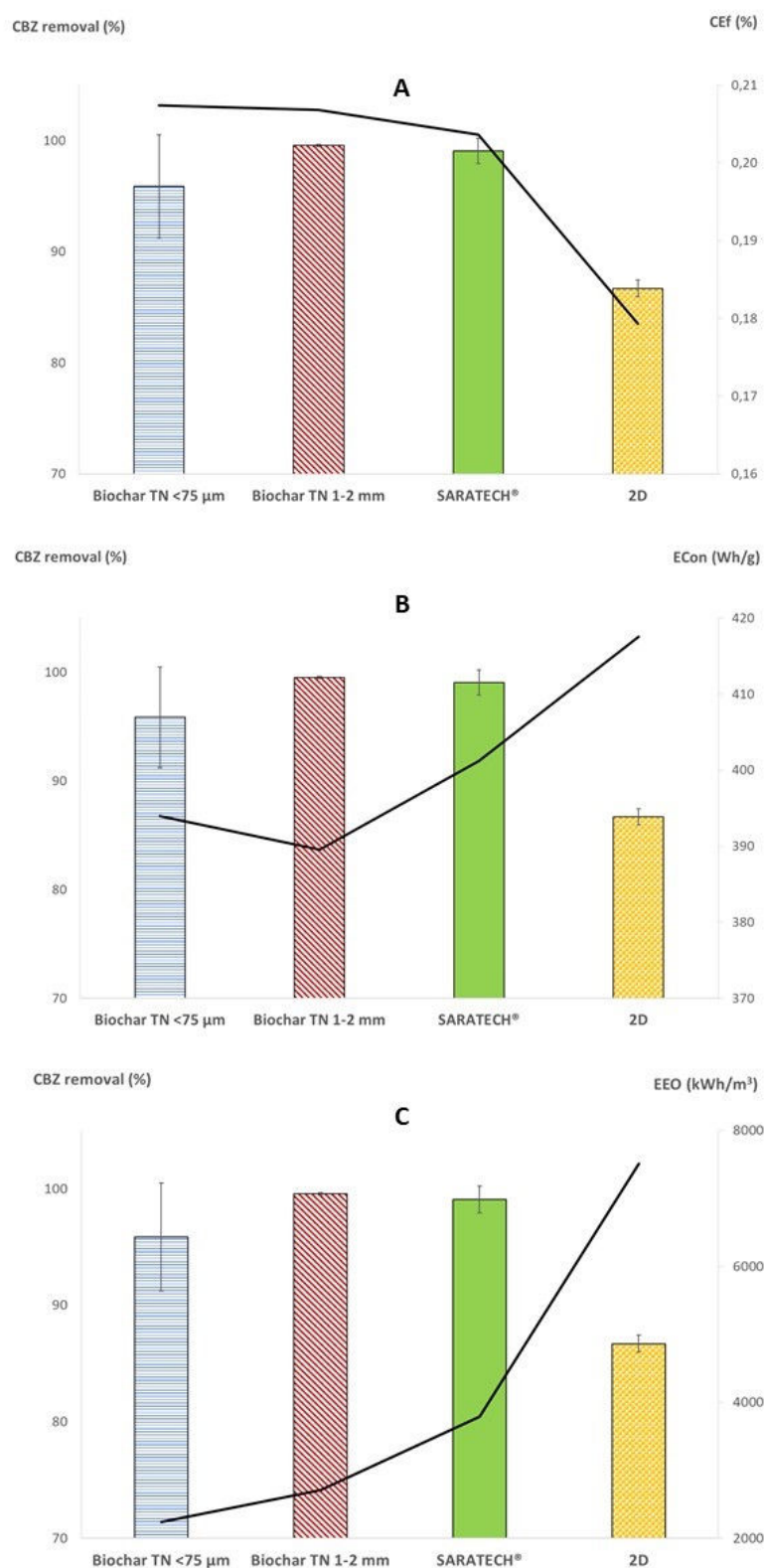


Figure 13. Effect of the particulate electrode on the removal of CBZ, represented by bars, and on energy consumption (A), current efficiency (B), and electric energy per order (C), represented by the black lines, and comparison between the 2D and the 3D process (operational conditions: $j = 6.67 \text{ mA/cm}^2$; $\text{NaCl} = 0.1 \text{ M}$; $\text{CBZi} = 10 \text{ mg/L}$; $\text{pH} = 7$; reaction time = 45 min; interelectrode distance = 7.5 cm; particulate electrode = 1 mg/mL solution; cathode = STS; anode = MMO).

Alighardashi et al. [34] reported a maximum current efficiency of 0.7% for the removal of CBZ in the 2D process (using 7.0 mA/cm² current density, 5 mg/L initial concentration of CBZ, 500 mg/L NaCl concentration, 60 min reaction time, and aluminum electrodes) and 16% for the 3D process (same experimental conditions except 0.5 g/L of activated carbon and a 10 min reaction time). The removal efficiency was 30 and 90% for the 2D and 3D processes, respectively. The calculated energy efficiency (evaluated through the electric energy per order) was 133,000 and 2520 kWh/m³ for the 2D and 3D processes, respectively.

Considering the obtained results, the 3D process allowed efficient removal of CBZ after a shorter period when compared with the 2D process, decreasing the energy consumption with higher current efficiency. The particulate electrode that presented the best performance when considering the energetic factors, kinetics, removal efficiency, and reaction time was the biochar TN 1–2 mm. Therefore, this biochar showed promising characteristics to be used as particulate electrode in 3D electrochemical processes to remove CBZ from wastewaters.

4. Conclusions

The 3D process was a more efficient process for CBZ removal than the 2D for all the tested adsorbents. The polarizability of the particulate electrodes of the 3D system was of higher importance than the adsorption capacity of the materials. The biochar TN 1–2 mm presented the best performance when considering the energetic factors, removal efficiency, and reaction time.

Biochars, which are low-cost and ecofriendly materials, have shown to be promising solutions, and may be a more sustainable and economic alternative than activated carbons.

Supplementary Materials: The following are available online at <https://www.mdpi.com/article/10.3390/app11146432/s1>, Figure S1: CBZ absorption spectra between 200 and 450 nm at different pH values during 60 min after solution preparation.

Author Contributions: Conceptualization, O.M.F., H.P.A.N. and S.A.F.; funding acquisition, A.J.R., C.M.O. and C.D.-M.; investigation, L.C.-S., C.S., M.M.M. and P.P.; methodology, L.C.-S. and C.S.; project administration, A.J.R., C.M.O. and C.D.-M.; resources, A.J.R., C.M.O. and C.D.-M.; supervision, O.M.F., H.P.A.N., A.J.R., C.M.O., S.A.F. and C.D.-M.; visualization, P.P.; writing—original draft, L.C.-S. and C.S.; writing—review and editing, O.M.F., M.M.M., H.P.A.N., M.C., P.P. and S.A.F. All authors have read and agreed to the published version of the manuscript.

Funding: This research was funded by the Associate Laboratory for Green Chemistry-LAQV, which is financed by national funds from FCT/MCTES (UIDB/50006/2020). This research also was funded through project OXI-e3D (POCI-01-0247-FEDER-039882), sponsored by the Program “Portugal 2020”, and cofunded by “Fundo Europeu de Desenvolvimento Regional (FEDER)” through POCI. M.M.M. is grateful for the financial support financed by national funds through FCT—Fundação para a Ciência e a Tecnologia, I.P., within the scope of the project CEECIND/02702/2017.

Institutional Review Board Statement: Not applicable.

Informed Consent Statement: Not applicable.

Data Availability Statement: Not applicable.

Acknowledgments: The supply of the vineyard prunings by Sogrape, S.A. and the biochar production by Ibero Massa Florestal is acknowledged.

Conflicts of Interest: The authors declare no conflict of interest.

References

1. Paíga, P.; Santos, L.; Delerue-Matos, C. Development of a multi-residue method for the determination of human and veterinary pharmaceuticals and some of their metabolites in aqueous environmental matrices by SPE-UHPLC-MS/MS. *J. Pharm. Biomed. Anal.* **2017**, *135*, 75–86. [[CrossRef](#)] [[PubMed](#)]
2. Klatte, S.; Schaefer, H.-C.; Hempel, M. Pharmaceuticals in the environment—A short review on options to minimize the exposure of humans, animals and ecosystems. *Sustain. Chem. Pharm.* **2017**, *5*, 61–66. [[CrossRef](#)]
3. Kümmerer, K. Pharmaceuticals in the Environment. *Annu. Rev. Environ. Resour.* **2010**, *35*, 57–75. [[CrossRef](#)]
4. Caban, M.; Stepnowski, P. How to decrease pharmaceuticals in the environment? A review. *Environ. Chem. Lett.* **2021**. [[CrossRef](#)]

5. Küster, A.; Adler, N. Pharmaceuticals in the environment: Scientific evidence of risks and its regulation. *Philos. Trans. R. Soc. Lond. B Biol. Sci.* **2014**, *369*, 20130587. [[CrossRef](#)]
6. Courtier, A.; Cadiere, A.; Roig, B. Human pharmaceuticals: Why and how to reduce their presence in the environment. *Curr. Opin. Green Sustain. Chem.* **2019**, *15*, 77–82. [[CrossRef](#)]
7. Wang, H.; Xi, H.; Xu, L.; Jin, M.; Zhao, W.; Liu, H. Ecotoxicological effects, environmental fate and risks of pharmaceutical and personal care products in the water environment: A review. *Sci. Total Environ.* **2021**, *788*, 147819. [[CrossRef](#)] [[PubMed](#)]
8. Li, W.C. Occurrence, sources, and fate of pharmaceuticals in aquatic environment and soil. *Environ. Pollut.* **2014**, *187*, 193–201. [[CrossRef](#)] [[PubMed](#)]
9. Babu, B.R.; Venkatesan, P.; Kanimozhi, R.; Basha, C.A. Removal of pharmaceuticals from wastewater by electrochemical oxidation using cylindrical flow reactor and optimization of treatment conditions. *J. Environ. Sci. Health A Tox. Hazard. Subst. Environ. Eng.* **2009**, *44*, 985–994. [[CrossRef](#)]
10. Sui, Q.; Cao, X.; Lu, S.; Zhao, W.; Qiu, Z.; Yu, G. Occurrence, sources and fate of pharmaceuticals and personal care products in the groundwater: A review. *Emerg. Contam.* **2015**, *1*, 14–24. [[CrossRef](#)]
11. Jurado, A.; Vázquez-Suñé, E.; Carrera, J.; López de Alda, M.; Pujades, E.; Barceló, D. Emerging organic contaminants in groundwater in Spain: A review of sources, recent occurrence and fate in a European context. *Sci. Total Environ.* **2012**, *440*, 82–94. [[CrossRef](#)] [[PubMed](#)]
12. McCance, W.; Jones, O.A.H.; Edwards, M.; Surapaneni, A.; Chadalavada, S.; Currell, M. Contaminants of Emerging Concern as novel groundwater tracers for delineating wastewater impacts in urban and peri-urban areas. *Water Res.* **2018**, *146*, 118–133. [[CrossRef](#)] [[PubMed](#)]
13. Ben Mordechay, E.; Tarchitzky, J.; Chen, Y.; Shenker, M.; Chefetz, B. Composted biosolids and treated wastewater as sources of pharmaceuticals and personal care products for plant uptake: A case study with carbamazepine. *Environ. Pollut.* **2018**, *232*, 164–172. [[CrossRef](#)]
14. Shi, C.; He, Y.; Liu, J.; Lu, Y.; Fan, Y.; Liang, Y.; Xu, Y. Ecotoxicological Effect of Single and Combined Exposure of Carbamazepine and Cadmium on Female Danio rerio: A Multibiomarker Study. *Appl. Sci.* **2019**, *9*, 1362. [[CrossRef](#)]
15. Wick, A.; Fink, G.; Joss, A.; Siegrist, H.; Ternes, T.A. Fate of beta blockers and psycho-active drugs in conventional wastewater treatment. *Water Res.* **2009**, *43*, 1060–1074. [[CrossRef](#)] [[PubMed](#)]
16. Bahlmann, A.; Brack, W.; Schneider, R.J.; Krauss, M. Carbamazepine and its metabolites in wastewater: Analytical pitfalls and occurrence in Germany and Portugal. *Water Res.* **2014**, *57*, 104–114. [[CrossRef](#)]
17. Zhang, Y.; Geißén, S.-U.; Gal, C. Carbamazepine and diclofenac: Removal in wastewater treatment plants and occurrence in water bodies. *Chemosphere* **2008**, *73*, 1151–1161. [[CrossRef](#)]
18. Hai, F.L.; Yang, S.; Asif, M.B.; Sencadas, V.; Shawkat, S.; Sanderson-Smith, M.; Gorman, J.; Xu, Z.-Q.; Yamamoto, K. Carbamazepine as a Possible Anthropogenic Marker in Water: Occurrences, Toxicological Effects, Regulations and Removal by Wastewater Treatment Technologies. *Water* **2018**, *10*, 107. [[CrossRef](#)]
19. Shenker, M.; Harush, D.; Ben-Ari, J.; Chefetz, B. Uptake of carbamazepine by cucumber plants—A case study related to irrigation with reclaimed wastewater. *Chemosphere* **2011**, *82*, 905–910. [[CrossRef](#)]
20. Gasca-Pérez, E.; Galar-Martínez, M.; García-Medina, S.; Pérez-Coyotl, I.A.; Ruiz-Lara, K.; Cano-Viveros, S.; Pérez-Pastén Borja, R.; Gómez-Oliván, L.M. Short-term exposure to carbamazepine causes oxidative stress on common carp (*Cyprinus carpio*). *Environ. Toxicol. Pharmacol.* **2019**, *66*, 96–103. [[CrossRef](#)] [[PubMed](#)]
21. Salgado, R.; Marques, R.; Noronha, J.P.; Carvalho, G.; Oehmen, A.; Reis, M.A.M. Assessing the removal of pharmaceuticals and personal care products in a full-scale activated sludge plant. *Environ. Sci. Pollut. Res.* **2012**, *19*, 1818–1827. [[CrossRef](#)] [[PubMed](#)]
22. Radjenovic, J.; Petrovic, M.; Barceló, D. Analysis of pharmaceuticals in wastewater and removal using a membrane bioreactor. *Anal. Bioanal. Chem.* **2007**, *387*, 1365–1377. [[CrossRef](#)]
23. Bellona, C.; Drewes, J.E.; Oelker, G.; Luna, J.; Filteau, G.; Amy, G. Comparing nanofiltration and reverse osmosis for drinking water augmentation. *J. AWWA* **2008**, *100*, 102–116. [[CrossRef](#)]
24. Comerton, A.M.; Andrews, R.C.; Bagley, D.M. The influence of natural organic matter and cations on the rejection of endocrine disrupting and pharmaceutically active compounds by nanofiltration. *Water Res.* **2009**, *43*, 613–622. [[CrossRef](#)]
25. Wert, E.C.; Rosario-Ortiz, F.L.; Snyder, S.A. Effect of ozone exposure on the oxidation of trace organic contaminants in wastewater. *Water Res.* **2009**, *43*, 1005–1014. [[CrossRef](#)] [[PubMed](#)]
26. Alharbi, S.K.; Kang, J.; Nghiem, L.D.; van de Merwe, J.P.; Leusch, F.D.L.; Price, W.E. Photolysis and UV/H₂O₂ of diclofenac, sulfamethoxazole, carbamazepine, and trimethoprim: Identification of their major degradation products by ESI-LC-MS and assessment of the toxicity of reaction mixtures. *Process Saf. Environ. Prot.* **2017**, *112*, 222–234. [[CrossRef](#)]
27. Shirazi, E.; Torabian, A.; Nabi-Bidhendi, G. Carbamazepine Removal from Groundwater: Effectiveness of the TiO₂/UV, Nanoparticulate Zero-Valent Iron, and Fenton (NZVI/H₂O₂) Processes. *Clean* **2013**, *41*, 1062–1072. [[CrossRef](#)]
28. Bernabeu, A.; Palacios, S.; Vicente, R.; Vercher, R.F.; Malato, S.; Arques, A.; Amat, A.M. Solar photo-Fenton at mild conditions to treat a mixture of six emerging pollutants. *Chem. Eng. J.* **2012**, *198–199*, 65–72. [[CrossRef](#)]
29. Kyzas, G.Z.; Fu, J.; Lazaridis, N.K.; Bikiaris, D.N.; Matis, K.A. New approaches on the removal of pharmaceuticals from wastewaters with adsorbent materials. *J. Mol. Liq.* **2015**, *209*, 87–93. [[CrossRef](#)]
30. Kårelid, V.; Larsson, G.; Björleinius, B. Pilot-scale removal of pharmaceuticals in municipal wastewater: Comparison of granular and powdered activated carbon treatment at three wastewater treatment plants. *J. Environ. Manag.* **2017**, *193*, 491–502. [[CrossRef](#)]

31. Skouteris, G.; Saroj, D.; Melidis, P.; Hai, F.I.; Ouki, S. The effect of activated carbon addition on membrane bioreactor processes for wastewater treatment and reclamation—A critical review. *Bioresour. Technol.* **2015**, *185*, 399–410. [[CrossRef](#)] [[PubMed](#)]
32. Grover, D.P.; Zhou, J.L.; Frickers, P.E.; Readman, J.W. Improved removal of estrogenic and pharmaceutical compounds in sewage effluent by full scale granular activated carbon: Impact on receiving river water. *J. Hazard. Mater.* **2011**, *185*, 1005–1011. [[CrossRef](#)] [[PubMed](#)]
33. Naghdi, M.; Taheran, M.; Pulicharla, R.; Rouissi, T.; Brar, S.K.; Verma, M.; Surampalli, R.Y. Pine-wood derived nanobiochar for removal of carbamazepine from aqueous media: Adsorption behavior and influential parameters. *Arab. J. Chem.* **2019**, *12*, 5292–5301. [[CrossRef](#)]
34. Alighardashi, A.; Agha, R.S.; Ebrahimzadeh, H. Improvement of Carbamazepine Degradation by a Three-Dimensional Electrochemical (3-EC) Process. *Int. J. Environ. Res.* **2018**, *12*, 451–458. [[CrossRef](#)]
35. GracePavithra, K.; Senthil Kumar, P.; Jaikumar, V.; SundarRajan, P. A review on three-dimensional electrochemical systems: Analysis of influencing parameters and cleaner approach mechanism for wastewater. *Rev. Environ. Sci. Bio/Technol.* **2020**, *19*, 873–896. [[CrossRef](#)]
36. Rajeshwar, K.; Ibanez, J.G.; Swain, G.M. Electrochemistry and the environment. *J. Appl. Electrochem.* **1994**, *24*, 1077–1091. [[CrossRef](#)]
37. Xu, L.; Zhao, H.; Shi, S.; Zhang, G.; Ni, J. Electrolytic treatment of C.I. Acid Orange 7 in aqueous solution using a three-dimensional electrode reactor. *Dyes Pigment.* **2008**, *77*, 158–164. [[CrossRef](#)]
38. Fernandes, M.J.; Moreira, M.M.; Paiga, P.; Dias, D.; Bernardo, M.; Carvalho, M.; Lapa, N.; Fonseca, I.; Morais, S.; Figueiredo, S.; et al. Evaluation of the adsorption potential of biochars prepared from forest and agri-food wastes for the removal of fluoxetine. *Bioresour. Technol.* **2019**, *292*, 121973. [[CrossRef](#)]
39. Lagergren, S. About theory of so-called adsorption of soluble substances. *Kongl. Vetensk. Acad. Handl.* **1898**, *24*, 1–39.
40. Ho, Y.S.; McKay, G. Pseudo-second order model for sorption processes. *Process Biochem.* **1999**, 451–465. [[CrossRef](#)]
41. Langmuir, I. The Adsorption of Gases on Plane Surfaces of Glass, Mica and Platinum. *J. Am. Chem. Soc.* **1918**, *40*, 1361–1403. [[CrossRef](#)]
42. Freundlich, H. Über die Adsorption in Lösungen. *Z. Phys. Chem.* **1907**, *57U*, 385–470. [[CrossRef](#)]
43. Bolton, J.R.; Bircher, K.G.; Tumas, W.; Tolman, C.A. Figures-of-merit for the technical development and application of advanced oxidation technologies for both electric- and solar-driven systems (IUPAC Technical Report). *Pure Appl. Chem.* **2001**, *73*, 627–637. [[CrossRef](#)]
44. Hu, X.; Yu, Y.; Sun, Z. Preparation and characterization of cerium-doped multiwalled carbon nanotubes electrode for the electrochemical degradation of low-concentration ceftazidime in aqueous solutions. *Electrochim. Acta* **2016**, *199*, 80–91. [[CrossRef](#)]
45. Chen, H.; Feng, Y.; Suo, N.; Long, Y.; Li, X.; Shi, Y.; Yu, Y. Preparation of particle electrodes from manganese slag and its degradation performance for salicylic acid in the three-dimensional electrode reactor (TDE). *Chemosphere* **2019**, *216*, 281–288. [[CrossRef](#)] [[PubMed](#)]
46. Lin, H.; Niu, J.; Xu, J.; Li, Y.; Pan, Y. Electrochemical mineralization of sulfamethoxazole by Ti/SnO₂-Sb/Ce-PbO₂ anode: Kinetics, reaction pathways, and energy cost evolution. *Electrochim. Acta* **2013**, *97*, 167–174. [[CrossRef](#)]
47. Yang, L.; Liang, L.; Wang, L.; Zhu, J.; Gao, S.; Xia, X. Accelerated photocatalytic oxidation of carbamazepine by a novel 3D hierarchical protonated g-C₃N₄/BiOBr heterojunction: Performance and mechanism. *Appl. Surf. Sci.* **2019**, *473*, 527–539. [[CrossRef](#)]
48. BIZI, M. Activated Carbon and the Principal Mineral Constituents of a Natural Soil in the Presence of Carbamazepine. *Water* **2019**, *11*, 2290. [[CrossRef](#)]
49. Gil, A.; Taoufik, N.; Garcia, A.M.; Korili, S.A. Comparative removal of emerging contaminants from aqueous solution by adsorption on an activated carbon. *Environ. Technol.* **2019**, *40*, 3017–3030. [[CrossRef](#)]
50. Teixidó, M.; Pignatello, J.J.; Beltrán, J.L.; Granados, M.; Peccia, J. Speciation of the Ionizable Antibiotic Sulfamethazine on Black Carbon (Biochar). *Environ. Sci. Biotechnol.* **2011**, *45*, 10020–10027. [[CrossRef](#)] [[PubMed](#)]
51. Dao, K.C.; Yang, C.-C.; Chen, K.-F.; Tsai, Y.-P. Recent Trends in Removal Pharmaceuticals and Personal Care Products by Electrochemical Oxidation and Combined Systems. *Water* **2020**, *12*, 1043. [[CrossRef](#)]
52. Zhang, C.; Jiang, Y.; Li, Y.; Hu, Z.; Zhou, L.; Zhou, M. Three-dimensional electrochemical process for wastewater treatment: A general review. *Chem. Eng. J.* **2013**, *228*, 455–467. [[CrossRef](#)]
53. Ghanbarlou, H.; Pedersen, N.L.; Fini, M.N.; Muff, J. Synergy optimization for the removal of dye and pesticides from drinking water using granular activated carbon particles in a 3D electrochemical reactor. *Environ. Sci. Pollut. Res.* **2020**, *27*, 22206–22213. [[CrossRef](#)] [[PubMed](#)]
54. Pedersen, N.L.; Fini, M.N.; Molnar, P.K.; Muff, J. Synergy of combined adsorption and electrochemical degradation of aqueous organics by granular activated carbon particulate electrodes. *Sep. Purif. Technol.* **2019**, *208*, 51–58. [[CrossRef](#)]
55. Gurung, K.; Ncibi, M.C.; Shestakova, M.; Sillanpää, M. Removal of carbamazepine from MBR effluent by electrochemical oxidation (EO) using a Ti-Ta₂O₅-SnO₂ electrode. *Appl. Catal. B* **2018**, *221*, 329–338. [[CrossRef](#)]